Research Article

Effect of Processing Route on the Surface Properties of Amorphous Indomethacin Measured by Inverse Gas Chromatography

D. J. Burnett,[1,5] J. Khoo,[2] M. Naderi,[2] J. Y. Y. Heng,[3] G. D. Wang,[3] and F. Thielmann[4]

Abstract. The aim of this study was to investigate the effect of processing route (i.e., quench cooling and ball milling) on the surface energy heterogeneity and surface chemistry of indomethacin (IMC). Recently developed inverse gas chromatography (IGC) methodology at finite concentrations was employed to determine the surface energy distributions of crystalline, quench cooled and milled IMC samples. Surface properties of crystalline and processed IMC were measurably different as determined by the IGC and other conventional characterization techniques: differential scanning calorimetry and powder X-ray diffraction. Quench cooled IMC was in fully amorphous form. Milled IMC showed no amorphous character by calorimetric or X-ray diffraction studies. It was demonstrated that both processed IMC samples were energetically more active than the crystalline IMC. In particular, milled IMC exhibited a relatively higher dispersive surface energy and higher surface basicity (electron donor capability). This may be attributed to the creation of surface defect sites or exposure of higher energy crystal facets during the milling process. This study confirms that processing route has notable influence on the surface energy distribution and surface acid–base character. IGC was demonstrated as a powerful technique for investigating surface properties of real-world, heterogeneous pharmaceutical materials.

KEY WORDS: heterogeneity; indomethacin; inverse gas chromatography; surface disorder; surface energy.

INTRODUCTION

Crystalline active pharmaceutical ingredients can become amorphous or disordered during different manufacturing processes either intentionally (i.e., spray-drying, freeze-drying, extrusion, *etc.*) or unintentionally (e.g., blending and micronization). Even though they may be produced *via* all above processing routes, these amorphous or disordered regions can be manifested throughout the entire crystal, affecting only the surface of the crystal, or even at localized points of the surface. Hence, the physical properties and ultimate behavior of these materials may vary dramatically (1). The changes in behavior subsequently can relate to difficulties in product formulation and even the final product attributes, such as wetting behavior during granulation of micronized drugs and performance variability in inhalation products.

Finite concentration inverse gas chromatography (IGC) experiments allow for the determination of surface energy distributions which more accurately describe the anisotropic surface energy for real materials. Several re-cent papers have utilized this relatively new methodology to understand the surface properties of pharmaceutical ingredients. For instance, the cohesive and bulk powder flow properties of lactose with and without a magnesium stearate lubricate were correlated to dispersive surface energy heterogeneity by IGC (2). Similar surface energy approaches were used to understand the mechanism of enhanced respiratory deposition of salbutamol sulfate when mixed with magnesium stearate (3). Additionally, IGC was used to measure the surface energy heterogeneity of lactose with the addition of fines used for pulmonary drug delivery (4). Further, the effect of surface energy heterogeneity was correlated to wet granulation properties for as-received and surface modified D-mannitol (5). Finite concentration IGC was also used to investigate the surface properties of micronized pharmaceutical materials (6). In all, surface energy analysis as measured by the recent finite IGC methods has become a powerful technique to investigate the surface properties of real-world, heterogeneous pharmaceutical materials.

In particular to milled pharmaceutical materials, there are several examples where IGC has been used to identify surface property changes. For instance, IGC was used to study the surface energies of crystalline, amorphous, and milled lactose (7). In this study, the amorphous (spray-dried) lactose has a significantly higher dispersive surface energy from the crystalline sample. Despite the milled lactose having a bulk

[1] Surface Measurement Systems, Ltd, 2125 28th Street SW, Suite 1, Allentown, Pennsylvania 18103, USA.
[2] Surface Measurement Systems, Ltd, Alperton, UK.
[3] Department of Chemical Engineering, Imperial College London, London, UK.
[4] Novartis PharmaAG, Basel, Switzerland.
[5] To whom correspondence should be addressed. (e-mail: burnett@smsna.com)

amorphous content of less than 1%, its dispersive surface energy was more consistent with that of the spray-dried, 100% amorphous sample, indicating amorphous regions are predominately located on the surface. Further, Ohta and Buckton (8) studied both dispersive surface energy and surface acidity/basicity as a function of milling time on cefditorenpivoxil. Longer milling times showed a strong correlation with increased surface basicity, attributed to increased dominance of surface carbonyl groups. Milling effects on the surface properties of form I paracetamol crystals was also studied by IGC (9). Dispersive surface energies for milled paracetamol decreased 20% with decreasing particle size. Also, milling increased the surface acidity, attributed to milling exposing a different dominant crystal facet. Finite concentration IGC experiments on needle-shaped D-mannitol crystals indicated that crystal fracture was dominated by geometric factors and not by the weakest attachment energy (10). Finally, IGC studies by Chamarthy and Pinal (11) revealed that the surface energy values of cryomilled samples were higher than those of the crystalline and amorphous (quench melt) counterparts for both felodipine and griseofulvin.

In this study, the dispersive and acid–base surface energy heterogeneity and Lewis acid–base properties of a model active pharmaceutical ingredient, indomethacin (IMC), were measured to investigate the effects of different processing routes on material surface properties. IMC was used as model compound for several studies regarding amorphism. It is an antipyretic and anti-inflammatory drug used in many pharmaceutical preparations (12,13). It has been proposed to have up to four polymorphic forms, though the metastable α- and stable γ-forms are the most commonly studied (14).

MATERIALS AND METHODS

Materials

IMC (>98% purity, γ-form) was provided by Novartis Pharmaceuticals Ltd. (Basel, Switzerland). Crystalline IMC was used as received (Fig. 1). Amorphous IMC was prepared by quench cooling. Approximately 0.150 g of as-received crystalline IMC was weighted into a circular aluminum weighing boat and was heated on a hotplate at a temperature above its melting point: 175°C. The sample was heated for about 5 min and until it was fully vitrified—with no apparent crystalline,
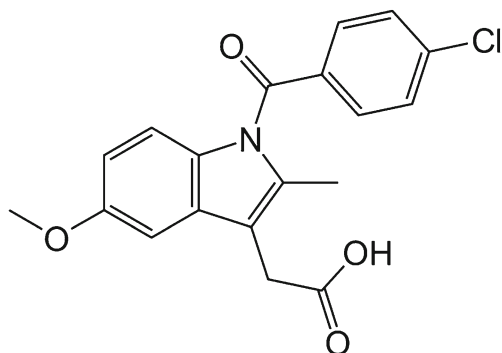

Fig. 1. Molecular structure of IMC

bubbles, or signs of decomposition. The glassy IMC was then ground gently into powder form using pestle and mortar.

As-received crystalline IMC was also subjected to milling using a ceramic ball mill apparatus. About 7 g of crystalline IMC and 20 ceramic balls (approximate 13.5 mm in diameter) were placed in a sealed 1L ceramic jar (mass ratio, 1:40). The ball mill apparatus was rotated on a Pascall Engineering 1600-VS-A roller mixer at a setting of 10 for a period of 2 h.

All samples were sieved to a particle size fraction of 90–106 μm to minimize any dependence on particle size and focus on differences in surface properties. Quench cooled and milled samples were kept in a desiccator filled with silica gel prior to any measurements. All measurements, including IGC experiments, were performed within 4 days from sample preparation. Caution was used to prevent sample relaxation between sample preparation and measurement (i.e., store at 0% RH and avoid exposure to high temperatures). However, it is possible for some changes to occur in the time scale from preparation to measurement.

Characterization Techniques

Powder X-ray diffraction (PXRD) was performed to confirm the presence of amorphous form and/or any disordered forms. PXRD diffractograms of all samples were obtained by using an X'Pert Pro diffractometer (PANalytical B.V., Almelo, The Netherlands). Samples were gently consolidated in a flat aluminum sample holder and scanned over an angular range of 5–60° (2θ) with a nickel-filtered Cu-Kα radiation generated at 40 kV and 40 mA. The gathered PXRD diffractograms were compared to the theoretical diffractograms, based on the crystal structures obtained from the Cambridge Crystallographic Data Centre.

Differential scanning calorimetry (DSC) experiments were also performed to confirm/exclude presence of amorphous or disordered forms. DSC measurements were performed immediately after quench cooling and milling as disordered IMC is known to be highly unstable, with a relatively low glass transition temperature (T_g) between 42°C and 45°C (15,16). About 8 mg of the sample was crimped in an aluminum DSC pan. Samples were heated from 25°C to 180°C at a ramping rate of 20°C/min, under a nitrogen gas flow of 50 mL/min. The calorimeter was calibrated with indium.

All surface energy analyses were carried out using iGC Surface Energy Analyzer (SMS, Alperton, UK) and the data were analyzed using both standard and advanced SEA Analysis Software. The injection system used by the iGC SEA allows the precise control of the injection size, therefore different amount (mole, n) of probe vapor can be chosen to pass through the sample column to achieve different surface coverages, n/n_m. If a series of probe vapors is injected at the same surface coverage, the surface energy and Gibbs specific free energy values can be determined. Consequently, the injections of probe vapors at different surface coverages will result in a distribution of surface energy as a function of surface coverage, which is referred as a surface energy profile. The determination of surface energy heterogeneity by iGC SEA can, therefore, be described as a mapping technique. Detailed methodology has been described elsewhere (1,5).

For all experiments, approximately 500 mg of each sample were packed into individual silanized glass columns (300 mm long by 4 mm inner diameter) using the SMS Column Packing Accessory. Each column was conditioned for a period of 2 h at 30°C and 0% RH with helium gas prior to any measurements. All experiments were conducted at 30°C with 10 sccm total flow rate of helium gas, using methane for dead volume corrections. Samples were run at a series of surface coverage with *n*-alkanes (decane, nonane, octane, and heptane; Aldrich, HPLC grade) and polar probe molecules (acetone, ethanol, acetonitrile, ethyl acetate, and dichloromethane; Aldrich, HPLC grade) to determine the dispersive surface energy as well as the specific free energies of adsorption, respectively. The complete IGC experiment over all surface coverages measured takes approximately 24 h for one sample. Repeat experiments were completed in succession on the same column to investigate if the elapsed time or exposure to vapors caused any measureable surface changes. Dispersive surface energy values were repeatable within ± 0.8 mJ/m^2 and acid–base surface energy values were repeatable within ± 0.4 mJ/m^2.

For the analysis, the method of Dorris and Gray was employed for the dispersive surface energy component (17). For the specific free energies of desorption, the Polarization approach was employed (18). Acid–base surface energy components were determined using the Good-van Oss–Chaudhury (GvOC) model (19,20) where the acid–base (γ_s^{AB}) component is taken as the geometric mean of the Lewis acid parameter (γ_s^-) and Lewis base parameter (γ_s^+).

The Gutmann acid–base theory was used to determine K_b (base, electron donor) and K_a (acid, electron acceptor) values (21). According to Gutmann, water is more acidic which contrasts with the GvOC approach where they assume that water is equally amphoteric (i.e., acid number equals base number). Therefore, the Gutmann model often yields a more accurate representation of the relative surface acidity and basicity. The Gutmann acid–base model using IGC has been applied to several pharmaceutically relevant studies (8,9,22,23). For a more detailed discussion on the application of the Gutmann acid–base theory using IGC, the reader is directed to the review article by Mukhopadhyay and Schreiber (24).

The Gutmann theory specifies using specific enthalpies of sorption (ΔH^{SP}). In this study, for simplicity specific free energy values (ΔG^{SP}) values were only measured at one temperature, thus enthalpies were approximated by the measured free energy values. This only holds true if entropy is small compared to enthalpy (i.e., $\Delta H^{SP} \sim \Delta G^{SP}$). This is a relatively common practice in the pharmaceutical field (8,9,22,25). Since ΔH^{SP} values require IGC experiments at multiple temperatures, and this will take longer timescales of experiments (~24 h). Due to the relative instability of the milled and quench cooled IMC samples, the authors chose to perform experiments at one temperature only and used the ΔG^{SP} values with the Gutmann equations. However, the authors note that a more robust approach would be to use ΔH^{SP}.

RESULTS

PXRD

Figure 2 shows the PXRD diffractograms of the as-received crystalline IMC and processed IMC samples. Complete
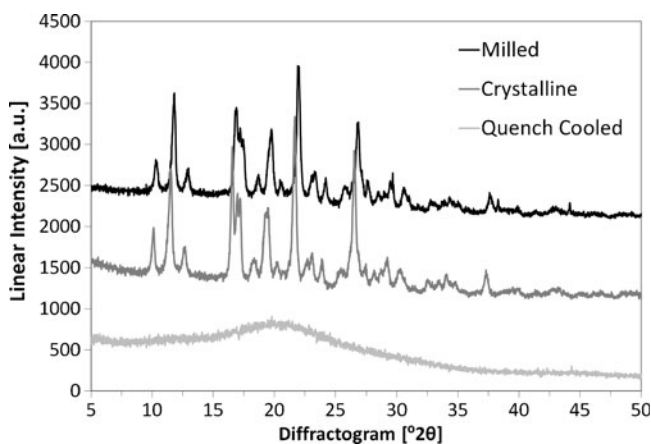

Fig. 2. PXRD diffractograms of crystalline form, ball-milled, and quench cooled IMC samples

absence of diffraction peaks in the diffractograms (amorphous halo) of quench cooled IMC revealed that the sample was completely amorphous. Milled IMC results show marginal decrease in intensity of the characteristic peaks, in particular over the range of angle 15° to 27° 2θ. It can also be observed here that milled IMC has remained predominantly in the original form of γ-IMC.

DSC

DSC thermograms of all samples are depicted in Fig. 3. Crystalline IMC (γ-form) shows a distinct endotherm as its melting peak, at temperature onset of 160°C. However, for milled IMC, there are multiple endotherms with between 154°C and 160°C. These features were observed in additional experiments on this sample, thus not considered to be an experimental error. For quench cooled IMC, the DSC thermograms exhibited an additional change in heat capacity at approximately 45°C, and an exothermic event in the range of 100–140°C. These thermal events can be associated with the T_g of IMC, and crystallization of amorphous IMC, respectively. The T_g value is in good agreement with previous studies (26). However, only
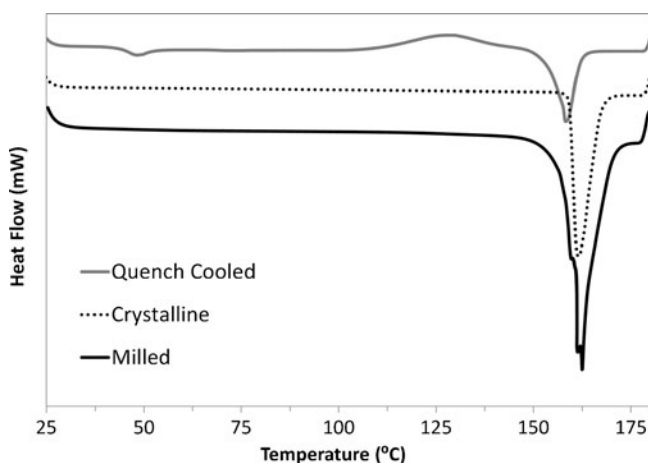

Fig. 3. Thermograms of crystalline form, ball-milled and quench cooled IMC samples

one melting peak was observed at 152°C onset, implying that quench cooled sample crystallized entirely into the α-IMC form.

Dispersive Surface Energy Heterogeneity

Dispersive (γ_s^D) surface energy profiles for the crystalline, milled, and quench cooled IMC samples are displayed in Fig. 4. γ_s^D profiles show that all IMC samples are energetically fairly heterogeneous—meaning the surface energy changes as a function of surface coverage. Milled IMC is evidently more active, having higher γ_s^D values across all surface coverages measured. This is followed by quench cooled IMC and crystalline IMC. It can be clearly observed that quench cooled and crystalline IMC samples possessed wider variations of γ_s^D, indicative of their more heterogeneous natures. Also, the curves in Fig. 4 indicate that the average γ_s^D values for the three samples obey the following trend: milled IMC>quench cooled IMC>crystalline IMC.

Acid–Base Surface Energy and Electron Donor-Acceptor Properties

The acid–base (γ_s^{AB}) component of the surface energy was determined using the Good-van Oss–Chaudhury approach and applying the Della Volpe scale (27). γ_s^{AB} profiles for the three IMC samples are displayed in Fig. 5. Crystalline IMC had marginally lower γ_s^{AB} values; meanwhile the milled and quench cooled samples have slightly higher acid–base surface energy values. Nonetheless, milled and quench cooled samples exhibit some variations in γ_s^{AB} across the surface coverages measured, even though the relative heterogeneity is not as pronounced as the ones shown in γ_s^D values. It is interesting to note that the quench cooled sample has the narrowest range of γ_s^{AB} values, compared to the other two samples. The γ_s^{AB} values for the crystalline and milled IMC are both broader than the quench cooled IMC. Average γ_s^{AB} values obey the same trends as γ_s^D values: milled IMC>quench cooled IMC>crystalline IMC.

Comparing with the γ_s^D component, γ_s^{AB} component of all samples contributes a minor part (up to about 7% polarity only) of the total surface energy, implying the low wettability of IMC samples, and hence concurring with the fact that IMC is a poorly water-soluble drug (28).
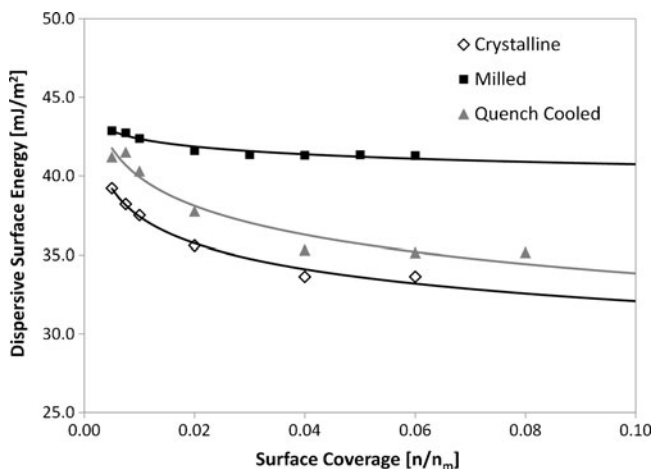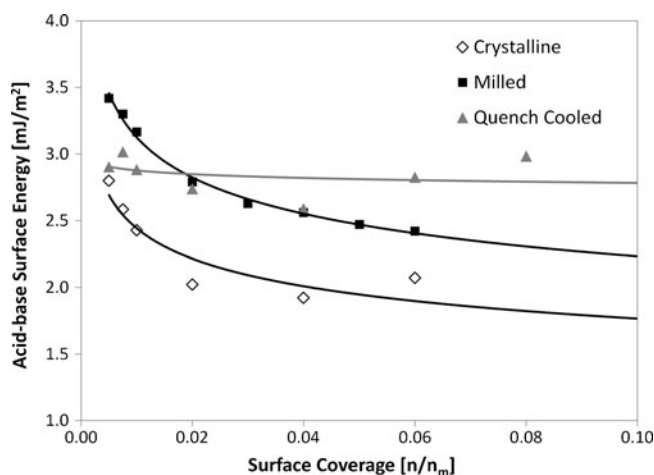

Fig. 5. Acid–base surface energy profiles of IMC samples

The Gutmann acid–base theory was applied to determine the electron donor–acceptor properties of the material surfaces, by the acid and base numbers (K_a and K_b). Gutmann theory accommodates the amphoteric nature of bipolar compounds, and is routinely used to characterize the surface chemistry of samples *via* IGC. These dimensionless K_a and K_b values were calculated by first measuring the ΔG^{SP} of acetone, ethanol, acetonitrile, ethyl acetate, and dichloromethane at each surface coverage. The ΔG^{SP} profiles as a result of the interactions with all five polar probe molecules for crystalline IMC are displayed in Fig. 6. Similar curves were generated for quench cooled and milled IMC. Crystalline IMC shows a degree of interaction with all five polar probes, but predominantly interact with acetonitrile and ethanol probes. Acetonitrile and ethanol are bifunctional probes, with the former being slightly basic and the latter being slightly acidic. Stronger interaction with these probes implies that the material surfaces are amphoteric in nature. The rank order shown in Fig. 6 for ΔG^{SP} interactions is similar for all three IMC samples.

Despite the approximation of ΔH^{SP} by ΔG^{SP} with the Gutmann acid–base approach applied in this study, the resulting acid–base values are still valuable for looking at trends between samples. For instance, Fig. 7 shows that all
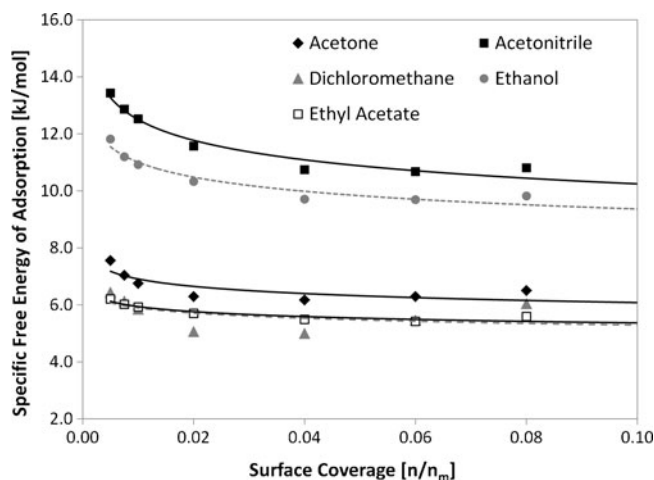

Fig. 4. Dispersive surface energy profiles of IMC samples

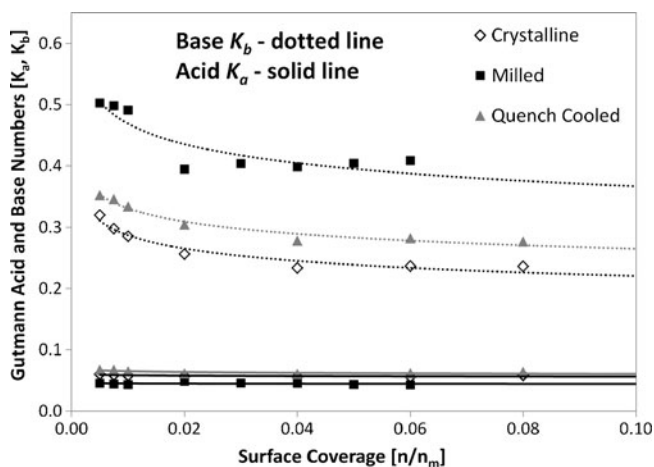**Fig. 6.** Specific free energy profiles of different polar probes with crystalline IMC

Fig. 7. Gutmann acid and base number profiles of IMC samples

samples have higher K_b than K_a across the entire surface coverage range measured, indicating that IMC surfaces are more basic in nature. This also shows that all surfaces possess higher concentration of electron-donating functional groups.

DISCUSSION

PXRD diffractograms and DSC thermograms of the quench cooled sample indicate the sample is completely amorphous, within detection limits. In contrast, the PXRD and DSC results for the as-received sample indicate a purely crystalline form (γ form). For the milled sample, the results are more complicated. The PXRD diffractogram for the milled IMC sample indicates a minor reduction in crystallinity, which is most likely due to surface disorder induced from the milling process. It was reported that mechanical activation by ball milling for much longer times ($\sim$6 h) resulted in formation of amorphous form *via* solid phase transformation (14). Further, the DSC thermogram for the milled IMC sample (Fig. 3) shows multiple endotherms (between 154°C and 160°C). These have been previously assigned to the melting peaks of metastable α- and stable γ-form of IMC polymorphs (29,30), but there was no evidence of α-IMC in the PXRD results. Therefore, it is possible that milling generated regions that convert to other forms when heated in the DSC experiment. Combined, these results indicate that the crystalline, quench cooled, and milled IMC samples have unique surface properties. The nature of these differences is further discussed below in regards to the surface energy heterogeneity results.

Dispersive surface energy profiles indicate that all three samples are energetically heterogeneous. Even crystalline samples can be energetically anisotropic. This is attributed to different crystal facets having different surface energies and has been observed previously on several different materials (1,31,32). Fairly homogeneous surfaces would result in a flat line for the surface energy profile. This phenomenon has been observed previously for surface modified D-mannitol crystals (20).

Between the three samples, the as-received crystalline IMC had the lowest dispersive surface energy values across the entire range of coverages measured. Quench cooled IMC had intermediate dispersive surface energy values, with milled IMC having the highest dispersive surface energy values.

Clearly, milling and quench cooling increase the dispersive surface energy. Surface energy values are inherently independent of surface area, particle size, and particle shape. From a theoretical standpoint, changes in surface roughness alone will not affect surface energy values. However, the orientation and interaction of IGC probe molecules can vary slightly if surface roughness is of the same magnitude of the molecular probe diameters (i.e., $\sim$5–10 Å). Therefore, surface roughness effects on measured surface energy values measured by IGC cannot be completely dismissed. Overall, the measured increased surface energy is not likely due to structural variations, but rather dominated by a change in the density or type of functional groups orientated on the surface. As mentioned earlier, there was little evidence of any bulk amorphization in milled IMC from PXRD and DSC results. Therefore, the higher surface energy values on milled surfaces could be due to formation of defect sites, kinks, steps, *etc.* or exposure of higher energy crystal facets during the milling process. For instance, milling exposed different crystalline planes in paracetamol due to fracturing along the plane with lowest attachment energy (9). For micronized ibipinabant, the dispersive surface energy values as measured by IGC increased with increasing milling energies, where the increased values were attributed to the generation of new higher energy sites. Further, dispersive surface energy values for milled lactose (1,7), griseofulvin (10), and felodipine (10) were measurably higher than their crystalline counterparts. In fact, several studies showed that the milled sample had higher dispersive surface energies than quench cooled or spray-dried amorphous reference materials (7,10), where the authors attributed the high surface energy values to surface crystal lattice defects. These results are consistent with the current study on IMC. There is a possibility that the milled sample could contain small surface amorphous regions that are below the detection limits of the PXRD and DSC experiments. However, the data in this study is consistent with previous research that suggests the high surface energy values are due to surface crystal lattice defects.

Milled IMC has a higher average value, but a slightly narrower range of values measured. The difference in surface energy between the minimum and maximum values determined is only ~5.1 mJ/m^2 ($\gamma_{s\,min}^D$39.3 mJ/m^2, $\gamma_{s\,max}^D$44.4 mJ/m^2). The quench cooled IMC had the broadest range of dispersive surface energy values ~8.8 mJ/m^2 ($\gamma_{s\,min}^D$34.8 mJ/m^2, $\gamma_{s\,max}^D$43.6 mJ/m^2), while the crystalline IMC had an intermediate variation of dispersive surface sites ~7.6 mJ/m^2 ($\gamma_{s\,min}^D$33.8 mJ/m^2, $\gamma_{s\,max}^D$41.4 mJ/m^2). Clearly, the different processing routes create surfaces of different surface properties.

Similarly, acid–base surface energy values indicate the quench cooled and milled IMC samples have higher γ_s^{AB} values compared to the crystalline sample which possesses a 16% of reduction in average γ_s^{AB} value. Between the milled and quench cooled IMC samples the differences in acid–base surface energy are more subtle. The acid–base surface energy values indicate a more uniform distribution of acid–base surface groups for the quench cooled sample compared to the milled IMC. However, the average acid–base surface energy value for quench cooled IMC is slightly higher than the milled IMC. Although the absolute differences between the γ_s^{AB} values are small, the trends suggest that the acid–base surface groups are altered by the processing conditions. Overall, the

differences in γ_s^{AB} values between the three samples are minimal and measured values are most likely dominated by the acid–base properties of IMC itself. Further differences in surface acid–base properties measured using the Gutmann theory are described below.

All IMC samples have higher ΔG^{SP} values with acetonitrile and ethanol probe molecules, implying an amphoteric nature of the material surfaces. Gutmann K_a and K_b values are a measure of Lewis acidity (electron acceptor) and basicity (electron donor), respectively. Changes in Gutmann acid–base values have been previously related to variations in powder processing behavior or product performance since they can cause differences in triboelectric charging (33), powder flow (34), and other surface and powder properties (35,36). The K_a and K_b values in Fig. 7 clearly depict that crystalline IMC has the lowest electron donor values, followed by the quench cooled sample which has marginally higher electron donor values. The milled IMC has the highest electron donor values, and lowest electron acceptor values. Milling of cefditorenpivoxil showed a strong increase in Gutmann surface basicity with increasing milling times (8), while Gutmann surface acidity increased with decreasing particle size (i.e., increased milling) for paracetamol (9). Together with the surface energy values, these acid–base results reveal the complex nature of surface property changes associated with milling.

CONCLUSION

Surface properties of Indomethacin with different processing routes were investigated. Quench cooling and milling both produced surface properties that were measurably different from crystalline IMC as determined by IGC, DSC, and PXRD. Crystalline IMC had the lowest surface energy values. There was no clear DSC or PXRD evidence of any measurable amorphous content in the milled IMC sample, but it had the highest surface energy values and highest surface basicity (electron donor capability). This is most likely due to the creation of surface defect sites. Quench cooled IMC showed clear evidence of high amorphous contents by PXRD and had intermediate dispersive surface energy values.

REFERENCES

1. Thielmann F, Burnett DJ, Heng JYY. Determination of the surface energy distributions of different processed lactose. Drug Dev & Ind Pharm. 2007;33:1240–53.
2. Zhou Q, Denman JA, Gengenbach T, Das S, Qu L, Zhang H, Larson I, Stewart PJ, Morton DAV. Characterization of the surface properties of a model pharmaceutical find powder modified with a pharmaceutical lubricant to improve flow *via* a mechanical dry coating approach. J Pharm Sci. 2011;100:3421–30.
3. Tay T, Das S, Stewart P. Magnesium stearate increases salbutamol sulphate dispersion: What is the mechanism? Int J Pharm. 2010;383:62–9.
4. Ho R, Muresan AS, Hebbink GA, Heng JYY. Influence of fines on the surface energy heterogeneity of lactose for pulmonary drug delivery. Int J Pharm. 2010;388:88–94.
5. Ho R, Dilworth SE, Williams DR, Heng JYY. Role of surface chemistry and energetics in high shear wet granulation. Ind Eng Chem Res. 2011;50:9642–9.
6. Gamble JF, Leane M, Olusanmi D, Tobyn M, Supuk E, Khoo J, Naderi M. Surface energy analysis as a tool to probe the surface energy characteristics of micronized materials—A comparison with inverse gas chromatography. M Int J Pharm. 2012;422:238–44.
7. Newell HE, Buckton G, Butler DA, Thielmann F, Williams DR. The use of inverse phase gas chromatography to measure the surface energy of crystalline, amorphous, and recently milled lactose. Pharm Res. 2001;18:662–6.
8. Ohta M, Buckton G. Determination of the changes in surface energetics of cefditorenpivoxil as a consequence of processing induced disorder and equilibration to different relative humidities. Int J Pharm. 2001;269:81–8.
9. Heng JYY, Thielmann F, Williams DR. The effects of milling on the surface properties of form I paracetamol crystals. Pharm Res. 2006;23:1918–27.
10. Ho R, Naderi M, Heng JYY, Williams DR, Thielmann F, Bouza P, Keith AR, Thiele G, and Burnett DJ, Effect of milling on particle shape and surface energy heterogeneity of needle-shaped crystals. Pharm. Res. in press
11. Chamarthy SP, Pinal R. The nature of crystal disorder in milled pharmaceutical materials. Colloid Surface A. 2008;331:68–75.
12. Shen TY, Windholz TB, Rosegay A, Witzel BE, Wilson AN, Willett JD, Holtz WJ, Ellis RL, Matzuk AR, Lucas S, Stammer CH, Holly FW, Sarett LH, Risely EA, Nuss GW, Winter CA. Non-steroid anti-inflammatory agents. J Am Chem Soc. 1963;85:488–9.
13. Winter CA, Risley EA, Nuss GW. Anti-inflammatory and antipyretic activities of indo-methacin, 1-(p-chlorobenzoyl)-5-methoxy-2-methyl-indole-3-acetic acid. J Pharmacol Exp Ther. 1963;141:369–76.
14. Borka L. Polymorphism of indomethacin—new modifications, their melting behavior and solubility. Acta Pharm Suec. 1974;11:295–303.
15. Planinsek O, Zadnik J, Kunaver M, Srcic S, Godec A. Structural evolution of indomethacin particles upon milling: time-resolved quantification and localization of disordered structure studied by IGC and DSC. J Pharm Sci. 2010;99:1968–80.
16. Karmwar P, Graeser K, Gordon KC, Strachan CJ, Rades T. Investigation of properties and recrystallisation behaviour of amorphous indomethacin samples prepared by different methods. Int J Pharm. 2011;417:94–100.
17. Dorris GM, Gray DG. Adsorption of n-alkanes at zero surface coverage on cellulose paper and wood fibers. J Colloid Interface Sci. 1980;77:353–62.
18. Donnet JB, Park SJ, Balard H. Evaluation of specific interactions of solid surfaces by Inverse Gas Chromatography: A new approach based on polarizability of the probes. Chromatographia. 1991;9–10:434–40.
19. Good RJ. In: Mittal KL, editor. Contact Angle, Wettability and Adhesion v3. Utrecht: VSP; 2003.
20. van Oss CJ. Interfacial Forces in Aqueous Media. New York: Marcel Dekker; 1994.
21. Gutmann V. The Donor-Acceptor Approach to Molecular Interaction. New York: Plenum; 1978.
22. Telko MJ, Hickey AJ. Critical assessment of inverse gas chromatography as means of assessing surface free energy and acid0base interaction of pharmaceutical powders. J Pharm Sci. 2007;96:2647–54.
23. Tong HHY, Shekunov BY, York P, Chow AHL. Influence of polymorphism on the surface energetics of salmeterol zinafoate crystallized from supercritical fluids. Pharm Res. 2002;19:640–8.
24. Mukhopadhyay P, Schreiber HP. Aspects of acid–base interactions and use of inverse gas chromatography. Colloid Surface A. 1995;100:47–71.
25. Ticehurst MD, Rowe RC, York P. Determination of the surface properties of two batches of salbutamol sulphate by inverse gas chromatography. Int J Pharm. 1994;111:241–9.
26. Savolainen M, Heinz A, Strachan C, Gordon KC, Yliruusi J, Rades T, Sander N. Screening for differences in the amorphous state of indomethacin using multivariate visualization. Eur J Pharm Sci. 2007;30:113–23.
27. Della Volpe C, Siboni S. Some reflections on acid–base solid surface free energy theories. J Colloid Interface Sci. 1997;195:121–36.
28. The Merck Index, 11th ed. New Jersey USA: Merck & Co., Inc.; 1989.

29. Crowley KJ, Zografi G. Cryogenic grinding of indomethacin polymorphs and solvates: Assessment of amorphous phase formation and amorphous phase physical stability. J Pharm Sci. 2002;91:492–507.

30. Bhugra C, Shmeis R, Krill SL, Pikal MJ. Different measures of molecular mobility: Comparison between calorimetric and thermally stimulated current relaxation times below Tg and correlation with dielectric relaxation times above Tg. J Pharm Sci. 2008;97:4498–515.

31. Heng JYY, Bismark A and Williams DR. Anisotropic surface chemistry of crystalline pharmaceutical solids. AAPS Pharm. Sci. Tech. 2006; 7: Article 84.

32. Ho R, Hinder SJ, Watts JF, Dilworth SE, Williams DR, Heng JYY. Determination of surface heterogeneity of D-mannitol by sessile drop contact angle and finite concentration inverse gas chromatography. Int J Pharm. 2010;387:79–86.

33. Ahfat NM, Buckton G, Burrows R, Ticehurst MD. An exploration of inter-relationships between contact angle, inverse phase gas chromatography and triboelectric charging data. Eur J Pharm Sci. 2000;9:271–6.

34. Feeley JC, York P, Sumby BC, Dicks H. Determination of surface properties and flow characteristics of salbutamol sulphate, before and after micronisation. Int J Pharm. 1998;172:89–96.

35. Mukhopadhay P, Schreiber HP. Aspects of acid–base interactions of inverse gas chromatography. Colloid Surface A. 1995;100:47–71.

36. Tong HHY, Shekunov BY, York P, Chow AHL. Characterization of two polymorphs of salbutamol xinafoate crystallized from supercritical fluids. Pharm Res. 2001;18:852–8.